Antiviral Research 170 (2019) 104556

Contents lists available at ScienceDirect

Antiviral Research

journal homepage: www.elsevier.com/locate/antiviral

A cross-reactive human monoclonal antibody targets the conserved H7 antigenic site A from fifth wave H7N9-infected humans

Mingxin Li[a,b], Li Chen[a,b], Qingguang Wang[a,b], Mengchan Hao[a,c], Xiaoqing zhang[a,b], Linlin Liu[d], Xiao Yu[d], Chunpeng Yang[a,b], Junqiang Xu[d,**], Jianjun Chen[a,c,***], Rui Gong[a,*]

[a] CAS Key Laboratory of Special Pathogens and Biosafety, Wuhan Institute of Virology, Chinese Academy of Sciences, Wuhan, Hubei, 430071, China
[b] University of Chinese Academy of Sciences, Beijing, 100049, China
[c] National Virus Resource Center, Wuhan Institute of Virology, Chinese Academy of Sciences, Wuhan, 430071, China
[d] Hubei Provincial Center for Disease Control and Prevention, Wuhan, 430079, China

ARTICLE INFO

Keywords:
Influenza virus
H7N9
Antibody
Hemagglutination inhibiting
Neutralizing
Epitope

ABSTRACT

Subtype H7 avian influenza viruses have been found to be associated with human infection and represent a risk for global public health. In 2013, the emergence of H7N9 virus in human beings and persistent human infection in China raised the most serious pandemic threat. Here we identified a human monoclonal antibody, P52E03, targeting the hemagglutinin (HA) of subtype H7 influenza viruses (H7 antigen), from a convalescent patient infected with H7N9 in 2017. P52E03 showed *in vitro* hemagglutination inhibiting (HI) and neutralizing activity against subtype H7 viruses belonging to both North American and Eurasian lineages. Moreover, it could prophylactically protect mice against weight loss and death caused by challenge with lethal H7N9 viruses *in vivo* and, therefore, is a candidate for development of antiviral agent against H7N9 infection. By generating escape mutant variants, we found that a single G151E substitution in the viral H7 antigenic site A could abort the neutralizing activity. Computational structural prediction of the P52E03/H7 complex revealed that residues including G151 in and around the conserved antigenic site A region are important for antigen recognition by the H7 cross-reactive antibody. Finally, we found that the P52E03 germline precursor (gHgL) antibody recognizes HA with measurable affinity, suggesting that its epitope is vulnerable to the human immune system and might elicit neutralizing antibodies (nAbs) *in vivo* after vaccination.

1. Introduction

Influenza virus is a serious global public health concern and infects both humans and animals. Within the past decades, subtype H7 avian influenza viruses have caused numerous outbreaks among poultry and increased number of human infections and thus are considered as a potential cause of pandemics [Abdelwhab et al., 2014]. Similarly to other subtypes of avian influenza viruses, subtype H7 influenza viruses are divided into two geographically distinct genetic lineages, North American and Eurasian [Banks et al, 2000]. Since 2000, H7N2 and H7N3 virus subtypes have caused human infections in North America [CDC, 2004a; 2004b; Tweed et al, 2004], and H7N2, H7N3 and H7N7 subtypes have been found in Europe [Fabiani et al, 2005; Koopmans et al, 2004; Nguyen-Van-Tam et al, 2006; Team, 2007].

In Asia, a novel reassortant avian-origin subtype H7N9 virus has been found to infect human beings in 2013 [Gao et al, 2013] and continues to cause human infections in China, resulting in 1567 cases with at least 615 deaths as of 5 September 2018 [WHO, 2018]. The 2016–2017 epidemic was the fifth wave and caused the largest number of human infections with 758 cases and 288 deaths [Su et al, 2017; WHO, 2017]. Importantly, highly pathogenic H7N9 viruses have emerged in the fifth wave [Ke et al., 2017]. Although refined antigenic epitopes on hemagglutinins (HAs) of the H7 subtype have not been well mapped, a computational analysis of H7 HAs identified five putative antigenic sites, A-E, on the HA head [Goff et al., 2013; Wiley et al, 1981]. Moreover, only site A is highly conserved within and between

* Corresponding author. CAS Key Laboratory of Special Pathogens and Biosafety, Wuhan Institute of Virology, Chinese Academy of Sciences, No.44 Xiao Hong Shan, Wuhan, Hubei, 430071, PR China.
** Corresponding author. Hubei Provincial Center for Disease Control and Prevention, No. 6 Zhuodaoquan North Road, Wuhan, Hubei, 430079, PR China.
*** Corresponding author. CAS Key Laboratory of Special Pathogens and Biosafety, Wuhan Institute of Virology, Chinese Academy of Sciences, No.44 Xiao Hong Shan, Wuhan, Hubei, 430071, PR China.
E-mail addresses: 609564945@qq.com (J. Xu), chenjj@wh.iov.cn (J. Chen), gongr@wh.iov.cn (R. Gong).

https://doi.org/10.1016/j.antiviral.2019.104556
Received 10 May 2019; Received in revised form 6 July 2019; Accepted 8 July 2019
Available online 09 July 2019
0166-3542/

North American and Eurasian lineages [Tan et al, 2016]. Despite no human H7N9 cases have been detected since March 2018, the subtype H7 viruses were still detected in birds and/or environmental samples [WHO, 2019]. As humans are immunologically naïve to subtype H7 viruses [Thornburg et al., 2016], it poses a long-term threat to public health, and requires multiple control strategies.

Currently, the main drugs used for antiviral treatment of H7N9 infection are the neuraminidase (NA) inhibitors, but they are most effective when administrated in early-stage infection [Aoki et al, 2003]. Additionally, the effectiveness of NA inhibitors may be limited because of the emergence of drug-resistant variants [Poland et al, 2009]. Vaccination is a prophylactic option for human H7N9 infection and several H7N9 vaccines have entered clinical trials [Bart et al, 2014; Fries et al, 2013; Jackson et al, 2015; Krammer et al, 2014; Mulligan et al, 2014]. Usually two doses of vaccine are required to induce detectable antibody titers in most participants [Jackson et al, 2015; Mulligan et al, 2014]. Since monoclonal neutralizing antibodies (mnAbs) exhibit promising potent as antiviral agents [Zhu et al, 2013], cross-reactive mnAbs to subtype H7 influenza viruses should be prepared to prevent or treat influenza early in a pandemic while vaccines and protective immunity are being developed [Sparrow et al, 2016].

In this study, the properties of an antibody P52E03, isolated from a convalescent patient infected in 2017, with cross-neutralizing activity against North American and Eurasian H7 influenza viruses, were characterized in HI and MN assay. *In vivo* studies with mice that were treated prophylactically with the antibody showed protection against weight loss and death following lethal H7N9 virus challenge. The results suggest that P52E03 would be a suitable prophylactic or/and therapeutic candidate against a potential pandemic.

2. Materials and methods

2.1. Ethics statement

This study was reviewed and approved by the Ethics Committee of the Wuhan Institute of Virology, Chinese Academy of sciences (WIVH34201901). Animal studies were performed in an animal biosafety level 2 facility. The experiments were performed in accordance with the Chinese national guidelines for the care of laboratory animals and were approved by the Animal Welfare and Ethical Review Committees of Wuhan Institute of Virology, Chinese Academy of Sciences (WIVA27201801).

2.2. Cells and viruses

Madin Darby Canine Kidney (MDCK) and 293T cells were obtained from the China Center for Type Culture Collection (CCTCC) and cultured in Dulbecco's modified Eagle's medium (DMEM) supplemented with 10% fetal bovine serum (FBS). A/Guangdong/17SF003/2016 (H7N9) (RKRTA-G) (r17SF/H7N9), A/chicken/Netherlands/2586/2003 (H7N7) (rNL03/H7N7), A/chicken/BC/CN006/2004 (H7N3) (rBC04/H7N3), and A/rhea/North Carolina/39482/93 (H7N1) (rNC93/H7N1) viruses with 2 surface genes of their own and 6 internal genes from A/Puerto Rico/8/34 (PR8) were rescued as previously described [Hoffmann et al, 2000]. A/Shanghai/02/2013 (H7N9) (rSH02/H7N9, 6:2 reassortant with PR8), A/Puerto Rico/8/34 (H1N1) (PR8/H1N1), A/Phalacrocorax_carbo/Hubei/HH179/2013 (H7N7) (HH179/H7N7), A/California/04/2009 (H1N1) (pdm09/H1N1), and A/Hubei/3/2005 (H3N2) (Hubei05/H3N2) viruses were inoculated into 10 day-old SPF embryonated chicken eggs to propagate. The H7N9 virus used in the animal study was NIBRG-267 which is a vaccine strain introduced from the National Institute for Biological Standards and Control (NIBSC) and adapted to mouse [Jie et al, 2016].

2.3. Cloning, expression and purification of the HA

Based on H3 numbering [Burke and Smith, 2014], cDNAs corresponding to residues 11–505 of the ectodomain of the HAs from A/Shanghai/2/2013 (H7N9) (SH02; GISAID database accession no. EPI138738) and A/Guangdong/17SF003/2016 (H7N9) (17SF; GISAID database accession no. EPI266963) were expressed in the baculovirus expression system and purified by metal affinity chromatography using Ni Sepharose Excel (GE Healthcare, Sweden) as previously described [Margine et al, 2013].

2.4. Phage-displayed Fab library construction

Peripheral blood mononuclear cells were isolated from convalescent patients 3 weeks after hospitalization. The anti-H7N9 human phage-display IgG-specific Fab library was constructed using previously described primers and methods with modifications [Zhu and Dimitrov, 2009]. The Fd (VH + CH1) fragments were obtained by a primary PCR with an IgG-CH1-Rev primer and separate VH FOR primers, and the intact Fab fragments were amplified through overlapping PCR with the flanking primers SfiF and IgG-SfiI-Rev.

2.5. Selection of H7-specific Fabs

The library was screened by sequential panning against SH02 HA for the first two rounds and 17SF HA for the third and fourth rounds. After each round of panning, the enrichment of antigen-specific phage was assessed by polyclonal phage enzyme-linked immunosorbent assay (ELISA). Positive clones were identified from the third and fourth rounds of panning by using monoclonal phage ELISA [Zhu and Dimitrov, 2009].

2.6. Expression and purification of Fab and IgG

Fab expression was performed in *E. coli* HB2151 bacterial culture according to the protocol in reference and purified on Ni-NTA column (Qiagen, Germany)[*Z.* Zhu and Dimitrov, 2009]. For conversion and preparation of IgG1, the heavy and light chains of Fabs were amplified and re-cloned into pVITRO2-neo-mcs (InvivoGen, USA). The IgG1 was expressed using the FreeStyle 293 expression kit following the manufacturer's protocol (Invitrogen, USA). The IgG1 was purified from the culture medium with a protein A column (GE Healthcare, Sweden).[Zhu et al, 2006].

2.7. Measurement of binding

ELISA was used for the first evaluation of binding. For human IgG binding, serially diluted antibodies were added and incubated for 2 h at 37 °C, HRP-conjugated goat anti-human IgG (Fc specific) antibody (sigma-Aldrich, USA) was used for detection. Enzymatic activity was measured with the subsequent addition of substrate ABTS (Life technology, USA), and absorbance signal was read at 405 nm.

In order to determine binding kinetics (affinity, K_D), biolayer interferometry was performed by using an Octet QK system (ForteBio, USA). rHAs were biotinylated with EZ-link®Sulfo-NHS-LC-Biotin (Pierce, USA), as per instructions and loaded onto Dip and Read Streptavidin (SA) Biosensors (ForteBio, USA). Antibodies of interest were measured by exposing sensors to four concentrations of each antibody. The readings from four sensors were aligned to the dissociation and globally fit for determining the K_D values, values with an R^2 close to 1 were considered acceptable.[Tan et al, 2016].

2.8. Hemagglutination inhibition (HI) and microneutralization (MN) assays

The ability of serum samples and mAbs to interfere with receptor

binding was measured by using an HI assay as previously descried [Klausberger et al, 2014; Liu et al, 2016]. Serum samples and mAbs were assessed by duplicate measurements. Serum samples were sequentially treated with 4 vol of receptor-destroying enzyme of *Vibrio cholera* filtrate (sigma-Aldrich, USA) and 1:20 (v/v) chicken red blood cells to remove nonspecific adsorption. 1% chicken red blood cell solution was added to the virus/serum or mAbs mixture to assay hemagglutination. The lowest concentration of mAb that was able to inhibit hemagglutination was considered as the HI endpoint concentration. The highest dilution of serum sample was considered as the final HI titer.

To assess the *in vitro* neutralization activity of the mAbs, we performed an MN assay [Huang et al., 2018a; Krause et al., 2012]. The mAbs (starting at 500 μg/ml) were two-fold serially diluted in triplicate, and mixed with an equal volume of viruses (50 μl of diluted mAbs plus 50 μl of virus) with a titer of 100 $TCID_{50}$ (50% tissue culture infective dose). After incubation for 1 h at RT, the mixture was added to MDCK cells and incubated for 72 h at 37 °C. The cell supernatants (50 μl/well) were transferred to 96-well V-bottom plates and incubated with 50 μl of a 1% chicken red blood cell solution for 30 min at RT to assay hemagglutination. The lowest concentration of mAb that was able to abolish the neutralizing activity was reported as the MN endpoint concentration which was different from IC_{50} but closer to IC_{90}. A minimum of three independent replicates were performed.

2.9. Generation of escape mutant variants

Escape mutant variants were generated by using previously described methods with modifications [Henry Dunand et al, 2016]. MDCK cells in 24-well plates were infected with 100 $TCID_{50}$ A/Shanghai/02/2013(H7N9) (rSH02/H7N9, 6:2 reassortant with PR8) virus for 1.5 h. After the incubation, medium supplemented with 1 μg/ml TPCK-trypsin (sigma-Aldrich, USA), with or without antibody at concentrations equivalent to 0.5, 1, and 2 MN endpoint concentrations, was added. Twenty-four hours post-infection (h.p.i.), supernatants were harvested and used to infect fresh cells that were overlaid again with medium supplemented with 1 μg/ml TPCK-trypsin, with or without the respective antibody, as described above. After six passages, the antibody concentration was doubled. Approximately three-fold concentration was used for passage 7 and 8. Viruses from passage 8 were plaque-purified and grown in 10-day-old embryonated chicken eggs for 72 h. The presence of the virus was confirmed using an HA assay. The HAs were then PCR-amplified and Sanger sequenced (TIANYI HUIYUAN, China).

2.10. Molecular modeling and docking

The amino-acid sequences of the mAbs heavy- and light-chain variable domains (V_H and V_L) were modeled by *PIGSPro* [Marcatili, 2008]. Both the “same antibody” and the “best heavy and light chains” approaches were tested. The crystal structure of HA protein from influenza H7N9 virus was obtained as PDB file 4n5k Xu et al., 2013, and the domain comprising amino acids 64 to 278 was selected for docking (H7 numbering starting from the first methionine). The starting positions were created using *PatchDock* servers, and the best starting position was chosen according to the residues of escape variants, using complementary-determining regions (CDRs) to recognize antigen and blocking the receptor binding [Schneidman-Duhovny et al., 2005]. Then, a local docking search by *Rosetta Docking 2 server* [Chaudhury et al, 2011; Sergey et al, 2013; Sergey and Gray, 2008] was performed for docking partners. The server returned 10 lowest-interface-energy structures, and the final structures were chosen from the top 3. The stereochemical qualities of the final model were validated with Molprobity [Huang et al., 2018a].

2.11. Prophylaxis and therapy in mice

To test the prophylactic *in vivo* protective effect of the mAb, passive transfer experiments were performed. Six week old female BALB/c mice (n = 6 per group) were injected intraperitoneally with 30, 10, or 2.5 mg/kg of mAb P52E03. Control mice received an irrelevant mAb (mAb NiV41-specific for Nipha virus) at 30 mg/kg. PBS-treated mice were used as a mock group. Twenty-four hours post transfer, mice were anesthetized (240 mg/kg avertin) and intranasally challenged with 10 murine lethal doses (mLD_{50}) of NIBRG-267 (H7N9). The weight of mice was monitored for 14 days and mice that had lost 25% or more of their initial body weight were scored dead and euthanized according to institutional guidelines. In a therapeutic setting, mice (n = 6) received a 10 mg/kg dose of mAb P52E03 24 h.p.i. Control mice received an irrelevant mAb as mentioned above at 15 mg/kg. The mice were monitored daily for survival and weight loss until day 14 post-infection.

3. Results

3.1. Generation of the H7-specific antibody P52E03 from natural H7N9 human infection

Three donors, P52, P71, and WHC001, were diagnosed with H7N9 influenza infection in 2017. Sera from convalescent donors were tested for antibodies against divergent H7 strains (Table 1). Sera from convalescent P52 and P71 patients showed a high HI titer (≥1280) against rSH02/H7N9, rNL03/H7N7 (Eurasian lineage) and rBC04/H7N3, rNC93/H7N1 (North American lineage). They also showed a high HI titer (640) against the wild bird virus HH179/H7N7. Serum from convalescent WHC001 patient showed a lower HI titer (160–320) against rSH02/H7N9, rNL03/H7N7, rNC93/H7N1, and a ≤20 HI titer against rBC04/H7N3 and HH179/H7N7. The three serum samples from convalescent patients and one serum sample from a healthy subject, BD001, showed strong HI titer (≥1280) against pdm09/H1N1 and < 20 HI titer against the seasonal influenza virus Hubei05/H3N2. As the sera showed cross-reactivities to divergent H7 viruses, we attempted to identify neutralizing monoclonal antibodies accounting for this ability.

To maximize the chances of selecting cross-reactive antibodies, we constructed two Fab phage-display libraries from donors P52 and P71 whose sera showed strong cross-reactive HI titers. After four rounds of panning, 760 colonies were picked randomly from the third and fourth rounds, and 185 positive Fab clones were identified. Sequence analysis

Table 1
HI titers of convalescent sera from donors with laboratory-confirmed H7N9 infection.

	P71[a]	P52	WHC001	BD001
rSH02/H7N9[c]	5120[b]	1280	160	20
rNL03/H7N7	1280	1280	160	20
rBC04/H7N3	2560	2560	20	20
rNC93/H7N1	2560	2560	320	20
HH179/H7N7	640	640	< 20	< 20
pdm09/H1N1	2560	1280	1280	1280
Hubei05/H3N2	< 20[d]	< 20	< 20	< 20

[a] Convalescent sera of P71, P52, and WHC001 donors were collected 21 days after hospitalization. BD001 was taken from a healthy subject as a negative control.

[b] HI titers were tested against divergent H7, H1, and H3 viruses. All measurements were performed in duplicate.

[c] rSH02/H7N9, A/shanghai/02/2013 (H7N9); rNL03/H7N7, A/chicken/Netherlands/2586/2003 (H7N7); rBC04/H7N3, A/chicken/BC/CN006/2004 (H7N3); rNC93/H7N1, A/rhea/North Carolina/39482/93 (H7N1); HH179/H7N7, A/*Phalacrocorax carbo*/Hubei/HH179/2013 (H7N7); pdm09/H1N1, A/California/04/2009 (H1N1); Hubei05/H3N2, A/Hubei/3/2005 (H3N2).

[d] The lowest dilution showed no inhibition hemagglutination was stated as < 20.

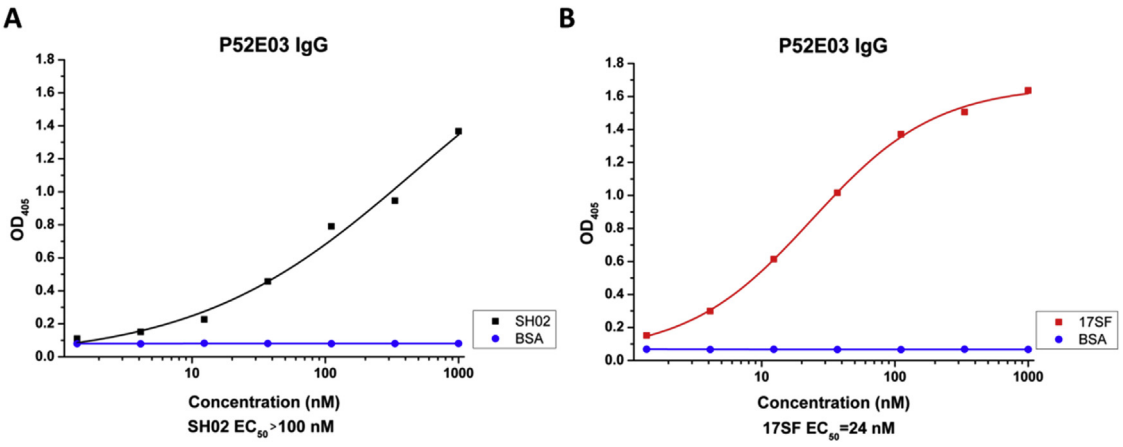

C

antigen	K_D (M)	K_{on}(1/Ms)	K_{dis}(1/s)	X^2	R^2
SH02	$1.57x10^{-7}$	$8.33x10^{3}$	$1.31x10^{-3}$	7.2400	0.991
17SF	$1.05x10^{-8}$	$1.01x10^{4}$	$1.06x10^{-4}$	0.0378	1.000

Fig. 1. Characterization of mAb P52E03. Binding characteristics of P52E03 IgG to recombinant SH02 HA (A) and 17SF HA (B) as measured by ELISA. (C) Binding kinetics of P52E03 as measured using an Octet QK system and recombinant HA (SH02, 17SF) as substrate. SH02, HA of A/shanghai/02/2013 (H7N9); 17SF, HA of A/Guangdong/17SF003/2016 (H7N9).

of these clones revealed 10 unique clones. Only one clone, P52E03, displayed both HI and MN activity.

The P52E03 Fab was then converted to IgG1 and its binding properties were characterized. P52E03 IgG1 exhibited stronger binding to the HA of the recent highly pathogenic H7N9 virus A/Guangdong/17SF003/2016 than to that of low pathogenic H7N9 virus A/shanghai/02/2013 as detected by ELISA (Fig. 1 A and B). Bio-layer interferometry was used to accurately measure P52E03 IgG1 affinity, detecting nanomolar K_D values, i.e., 157 nM for SH02 and 10.5 nM for 17SF (Fig. 1 C). Thus, the P52E03 mAb exhibited cross binding activity, suggesting its potential cross-reactivity with divergent H7 viruses.

3.2. P52E03 cross-reacts with divergent H7 viruses in HI and MN assays

The ability of P52E03 to interfere with HA binding to cell receptors was measured by an HI assay (Fig. 2A). mAbs were two-fold serially diluted from 1000 μg/ml. mAb 07-4B03 mHgL (chimeric antibody of 07–4B03) [Henry Dunand et al, 2016] which had high expression level and displayed similar HI titer with 07–4B03 against rSH02/H7N9 was used as a positive control (Fig. 2B). P52E03 showed an HI endpoint titer of 15.625–62.5 μg/ml against rSH02/H7N9, r17SF/H7N9, rNL03/H7N7 (Eurasian lineage) and rBC04/H7N3 (North American lineage), but weaker HI endpoint titer (125 μg/ml) against HH179/H7N7 (Eurasian lineage) and rNC93/H7N1 (North American lineage) (Fig. 2A). The control antibody 07-4B03 mHgL showed a similar behavior to P52E03 in these tested H7 strains (Fig. 2B).

To assay whether P52E03 exerted neutralizing activity *in vitro*, we performed a MN assay at a starting concentration of 500 μg/ml (Fig. 3). P52E03 showed high neutralizing activities with an MN endpoint titer of 3.9–10.4 μg/ml against rSH02/H7N9, rNL03/H7N7 (Eurasian lineage) and rBC04/H7N3, rNC93/H7N1 (North American lineage). Thus, P52E03 presents cross-HI and MN activity against divergent H7 viruses belonging to both North American and Eurasian lineages, suggesting that it was able to recognize a conserved epitope on the H7 head domain.

3.3. The human monoclonal antibody P52E03 targets a conserved H7 epitope

We then generated escape mutant variants of rSH02/H7N9, and determined the key residues recognized by P52E03. In addition, the broad-spectrum anti-stem neutralizing antibody CR9114 [Dreyfus et al., 2012] was selected for escape variants as a control. The single substitution G151E in HA was identified among the escape mutants of P52E03 (Fig. 4B). The D385G substitution in HA, in the antibody/antigen binding interface according to the crystal structure [Dreyfus et al., 2012], was observed in the CR9114 escape variants. P52E03 showed no HI or MN endpoint titer to its escape variant (Figs. 2A and 3F), whereas 07-4B03 mHgL, whose key residue has been reported as S152 (Fig. 4D) [Henry Dunand et al, 2016], showed high HI (7.81 μg/ml) and MN endpoint titer (20.8 μg/ml) to this escape variant (Figs. 2B and 3F). Both P52E03 and 07-4B03 mHgL showed strong HI (7.81–31.25 μg/ml) and MN endpoint titer (3.9–15.6 μg/ml) to the CR9114 escape variant (Fig. 2A, B, Fig 3G). Thus, the escape mutation of one antibody did not abort the binding of the others.

To further investigate the antibody epitope, we used a molecular docking-based strategy, which was verified by docking F10 or CR6261 antibodies to influenza virus HA and comparing with their X-ray structures [Pedotti et al, 2011]. The computationally predicated P52E03/H7 complex revealed that the antibody recognized residues in and around the conserved antigenic site A via three HCDRs (Fig. 4A and B), whereas only the long HCDR3 of 07–4B03 was involved (Fig. 4 C, D). Both antibodies could prevent virus binding to cell surface receptors. Sequence alignment showed that most of the residues in the epitopes of these two antibodies were largely overlapped and conserved between North American and Eurasian lineage strains (Fig. 5) which further proving that these two antibodies might be cross-reactive to subtype H7 viruses.

Among the 21 residues recognized by P52E03, based on molecular docking, the HA of A/Guangdong/17SF003/2016 (H7N9) contained only two substitutions, S136N and A143V, compared to the HA of A/shanghai/02/2013 (H7N9) (Fig. 5), and both residues might contribute

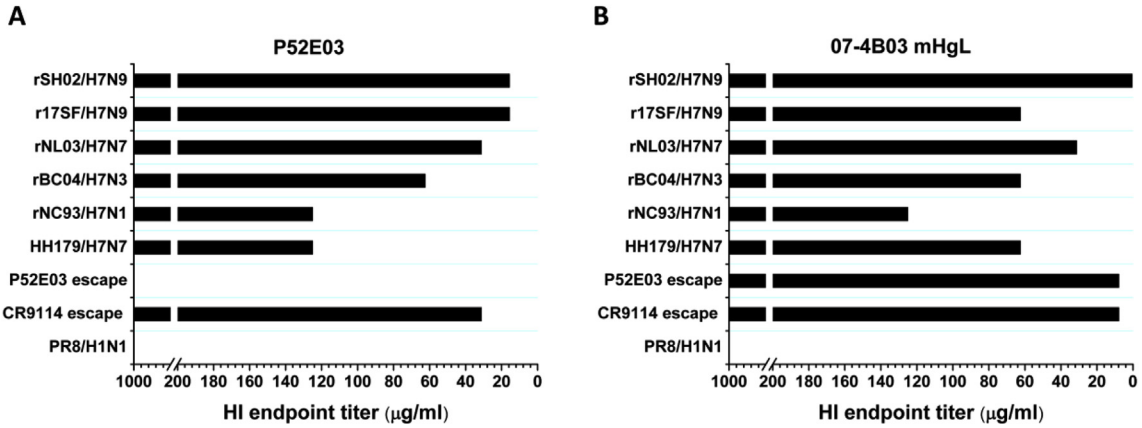

Fig. 2. HI activity of mAbs P52E03 and 4B03 mHgL. HI activity of antibody P52E03 (A) and 4B03 mHgL (B) to divergent H7 viruses. PR8/H1N1 was a negative control virus. mAbs were two-fold serially diluted from 1000 μg/ml. Minimum positive concentrations (μg/ml) are reported for HI endpoint titer. All measurements were performed in duplicate. The 4B03 mHgL antibody consisted of mature heavy chain and germline light chain derived from 07 to 4B03. rSH02/H7N9, A/shanghai/02/2013 (H7N9); r17SF/H7N9, A/Guangdong/17SF003/2016 (H7N9); rNL03/H7N7, A/chicken/Netherlands/2586/2003 (H7N7); rBC04/H7N3, A/chicken/BC/CN006/2004 (H7N3); rNC93/H7N1, A/rhea/North Carolina/39482/93 (H7N1); HH179/H7N7, A/*Phalacrocorax carbo*/Hubei/HH179/2013 (H7N7); PR8/H1N1, A/Puerto Rico/8/34 (H1N1). P52E03 escape, escape variant of P52E03 selected from rSH02/H7N9; CR9114 escape, escape variant of CR9114 selected from rSH02/H7N9.

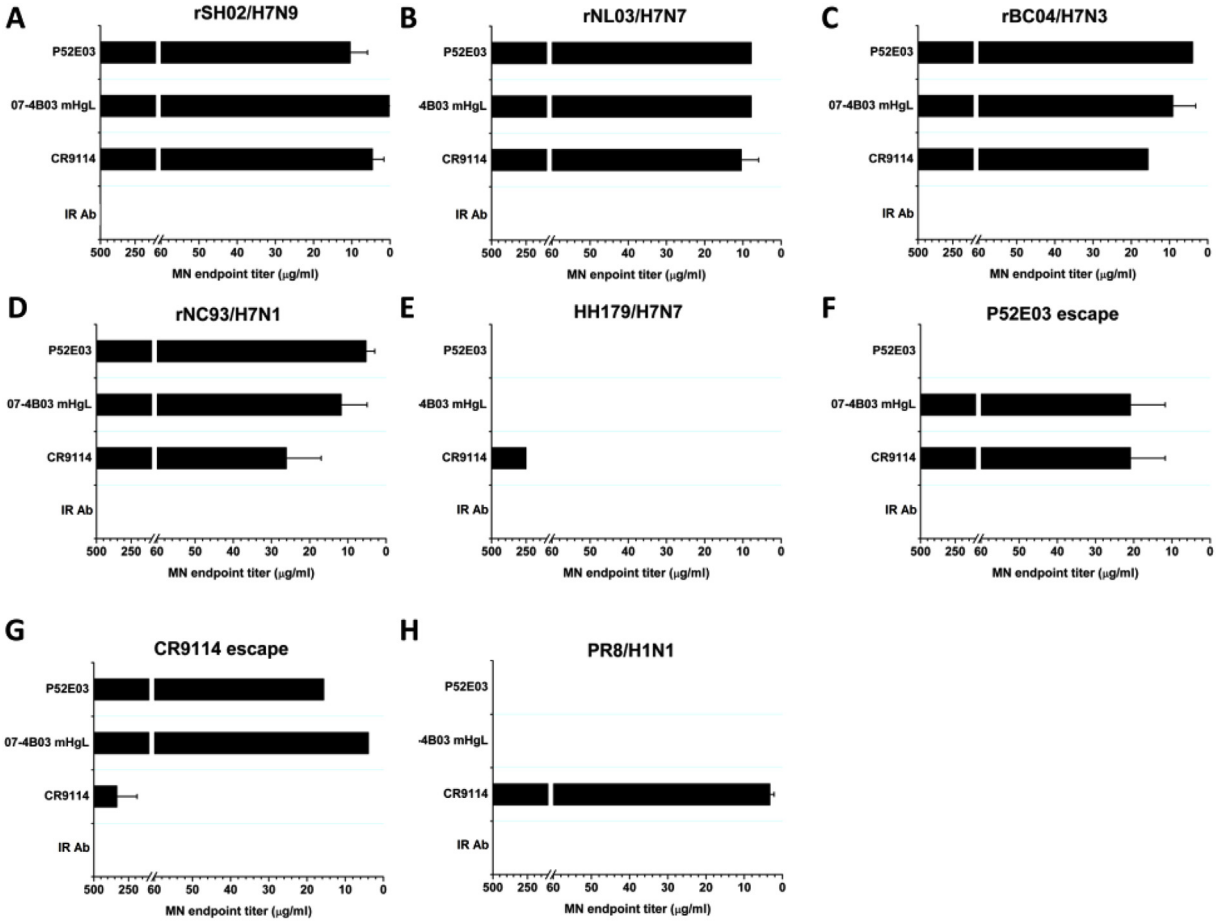

Fig. 3. MN activity of mAbs P52E03, 07-4B03 mHgL, and CR9114. (A, B) MN activity against Eurasian lineage strains. (C, D) MN activity against North American lineage strains. (F, G) MN activity against escape strains selected from rSH02/H7N9. (E) MN activity against Eurasian wild bird virus. (H) MN activity against PR8/H1N1. mAbs were two-fold serially diluted from 500 μg/ml, minimum positive concentrations in μg/ml are reported for MN endpoint titer. All measurements were performed in triplicate. rSH02/H7N9, A/shanghai/02/2013 (H7N9); rNL03/H7N7, A/chicken/Netherlands/2586/2003 (H7N7); rBC04/H7N3, A/chicken/BC/CN006/2004 (H7N3); rNC93/H7N1, A/rhea/North Carolina/39482/93 (H7N1); HH179/H7N7, A/*Phalacrocorax carbo*/Hubei/HH179/2013 (H7N7); PR8/H1N1, A/Puerto Rico/8/34 (H1N1). P52E03 escape, escape variant of P52E03 selected from rSH02/H7N9; CR9114 escape, escape variant of CR9114 selected from rSH02/H7N9. IR Ab: irrelevant antibody.

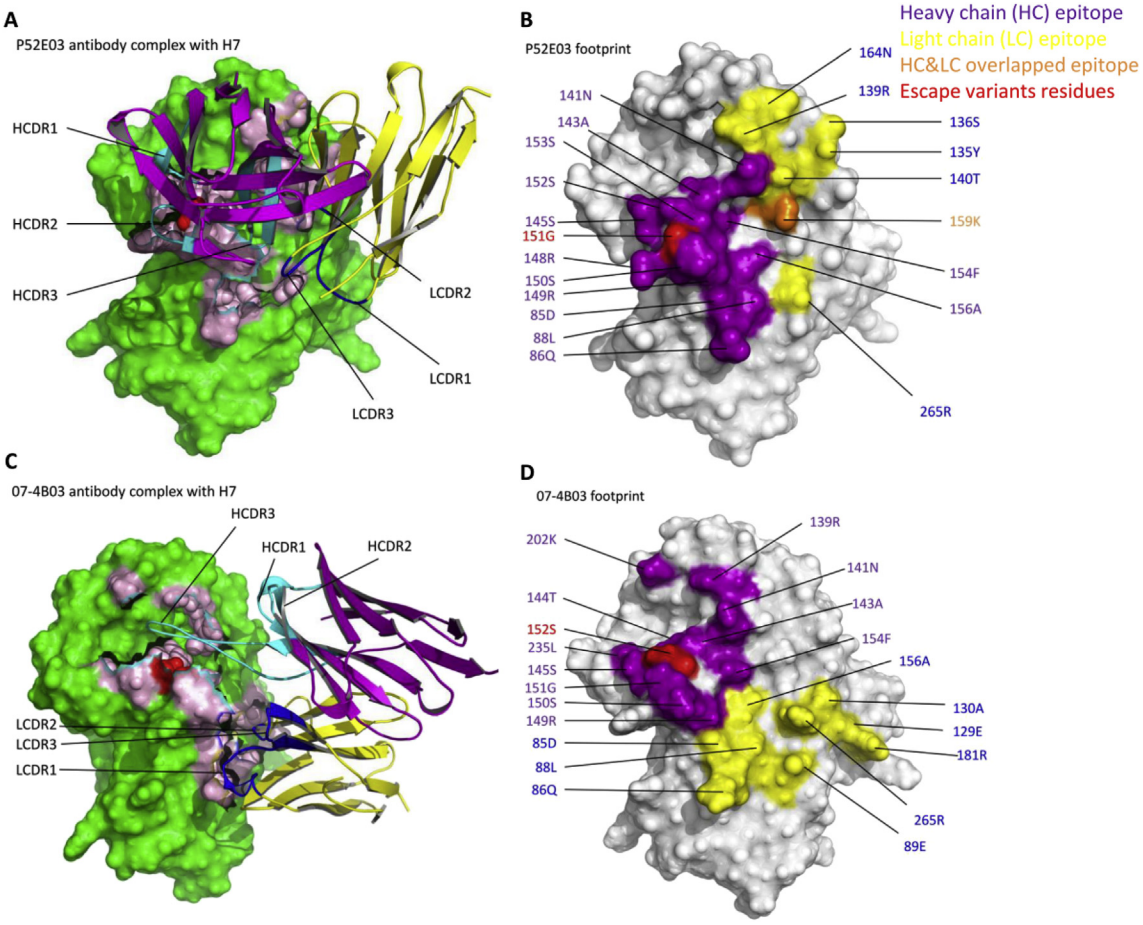

Fig. 4. Docking Structure of P52E03/H7, 07-4B03/H7 complexes. (A, C) Overall structures of P52E03/H7 (A) and 07-4B03/H7 (C) complexes, displayed in a cartoon representation. The single chain variable fragments (scFvs) of P52E03 and 07-4B03 (heavy chain in purple, light chain in yellow) bind the globular head domain of A/shanghai/02/2013 HA. The HA head domain is colored in green, and the epitope in light pink. (B, D) The footprints on H7 of scFv P52E03 (B) and 07-4B03 (D) are mapped on the HA surface. The epitope residues that are contacted by the heavy or light chain are colored in purple or yellow, respectively (all H7 numbering starting from the first methionine). The overlapping residues that contacted by both heavy and light chains are in orange. The residues found on the escape variants are in red. HC, heavy chain; LC, light chain; HCDR1-3, heavy chain CDRs 1–3; LCDR1-3, light chain CDRs 1–3.

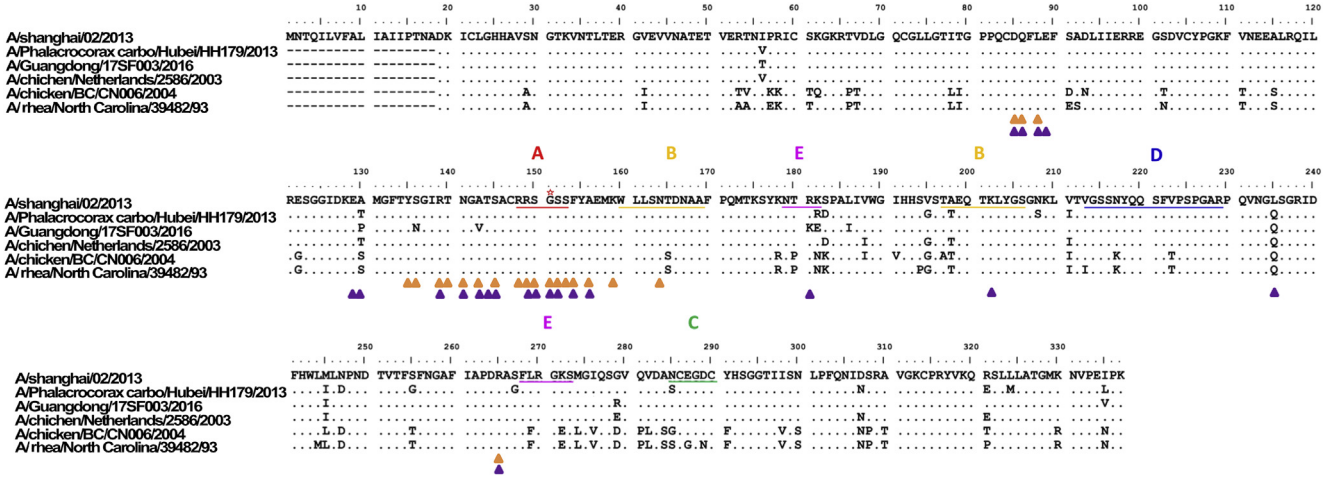

Fig. 5. Comparison of epitope residues recognized by P52E03 and 07-4B03 antibodies. HA residues recognized by P52E03 (orange triangles) and 07-4B03 (purple triangles) are mapped onto a sequence alignment of H7 HAs. Dots represent identical residues. Numbering is taken from the first methionine of H7. The five putative H7 antigenic sites are A (red), B (orange), C (green), D (blue), E (magenta). A/shanghai/02/2013, rSH02/H7N9; A/*Phalacrocorax carbo*/Hubei/HH179/2013, HH179/H7N7; A/Guangdong/17SF003/2016, r17SF/H7N9; A/chicken/Netherlands/2586/2003, rNL03/H7N7; A/chicken/BC/CN006/2004, rBC04/H7N3; A/rhea/North Carolina/39482/93, rNC93/H7N1.

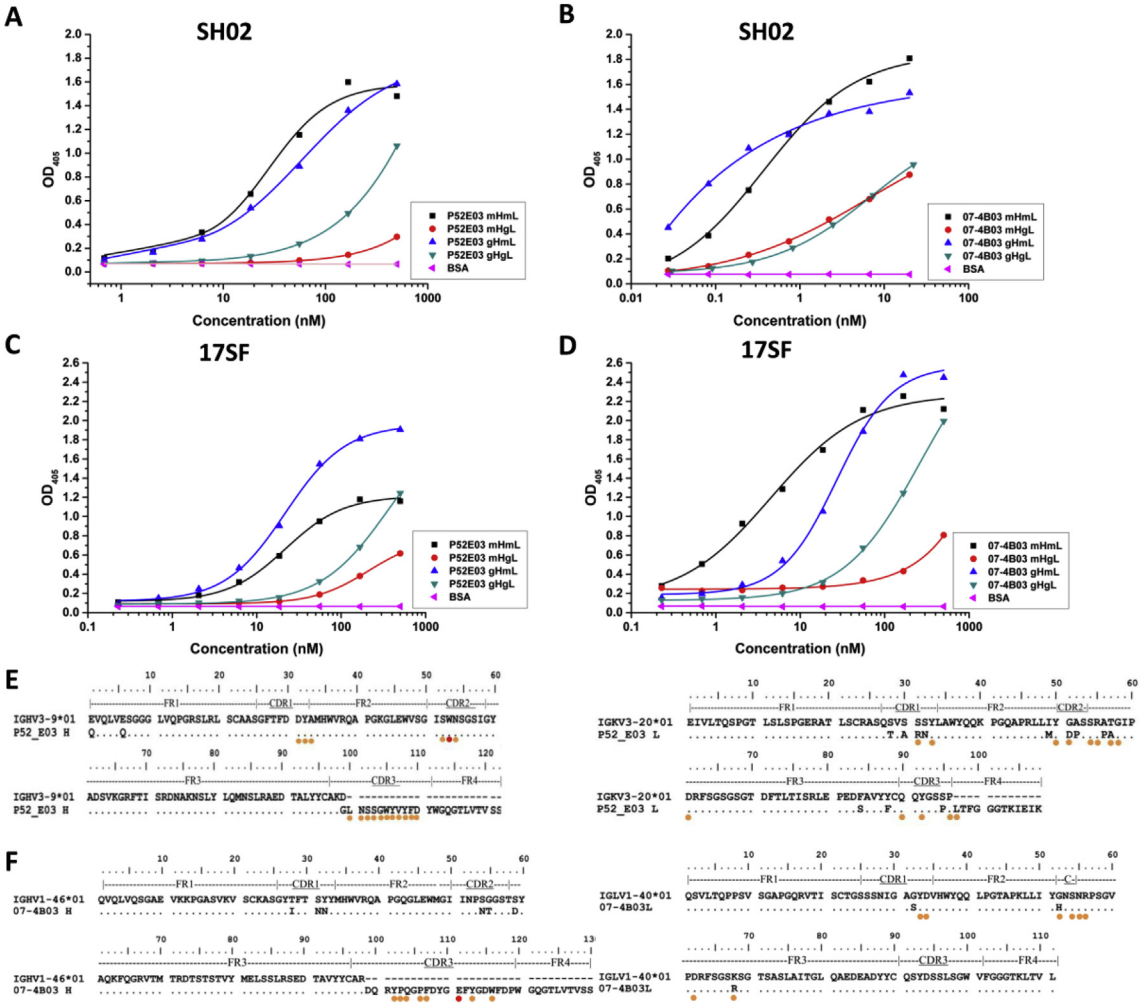

Fig. 6. Genetic and binding properties of antibodies. (A, B, C, D) ELISA binding of mature (mHmL), respective germline (gHgL), chimeric (mHgL, gHmL) forms of P52E03 (A, C) and 07-4B03 (B, D) to recombinant SH02 HA and 17SF HA. (E, F) Genetic characteristics of P52E03 (E) and 07-4B03 (F). The genetic features were determined using the international ImMunoGeneTics (IMGT) information system. The residues contacted by the SH02 HA antigen are marked by orange circles; those interacting with escape mutation residues are indicated by red circles. SH02, HA of A/shanghai/02/2013 (H7N9); 17SF, HA of A/Guangdong/17SF003/2016 (H7N9).

to the higher affinity of P53E03 to 17SF (Fig. 1C). Among the 770 H7N9 field strains isolated after September 2016, 700 showed simultaneous S136N and A143V substitutions, further proving that P52E03 might have a higher affinity to fifth-wave (e.g., A/Guangdong/17SF003/2016(H7N9)) than first-wave H7N9 viruses (e.g., A/shanghai/02/2013(H7N9)).

3.4. A germline precursor of the human monoclonal antibody P52E03 also binds recombinant HAs

To determine whether this conserved epitope is vulnerable to the human immune system [Xiao et al, 2009], we measured the binding properties of the P52E03 germline precursor (gHgL). Antibody 07-4B03 was selected as a control. Both germline precursors could bind HAs as soluble IgGs with measurable affinity (Fig. 6 A, B, C, D). Most likely, this was due to the fact that the conserved residues, in and around the H7 antigenic site A, were recognized by germline-like residues of the heavy chain (Fig. 6E, F). Thus, the epitope recognized by P52E03 might elicit nAbs *in vivo* after vaccination.

To define the molecular basis for the affinity maturation of the two antibodies, we determined the respective contribution of heavy and light chains to antigen recognition. To this end, we compared chimeric (mHgL, gHmL) and mature antibodies (mHmL). The chimeric gHmL of both antibodies bound to recombinant HAs with affinities similar to their respective mature mHmL (Fig. 6A, B, C, D). Thus, maturation of the heavy chain did not affect binding to recombinant HAs. However, maturation of the light chain alone mediated the increase in binding affinity. This finding suggested that light-chain somatic mutation is important for improving the binding and neutralization functions (Fig. 6 E, F).

3.5. The human monoclonal antibody P52E03 confers protection against lethal H7N9 virus challenge in prophylactic and therapeutic settings in the mouse model

To test the protective efficacy of P52E03 *in vivo*, we performed prophylactic and therapeutic passive transfer challenge experiments in the mouse model. In the prophylactic experiment, P52E03 was completely protective at 30 and 10 mg/kg. Under these conditions, no weight loss was observed, and the survival rate was 100%. However, in the group treated with 2.5 mg/kg antibody, mice lost nearly 20% of their initial body weight and the survival rate was only 33.3% (Fig. 7A). Thus, the prophylactic efficacy of P52E03 was dose-dependent. In the therapeutic experiment, mice treated with 10 mg/kg P52E03 started to lose weight soon after viral infection, undergoing a nearly 10% loss of initial body weight at day 5. Consistently, the survival rate was only

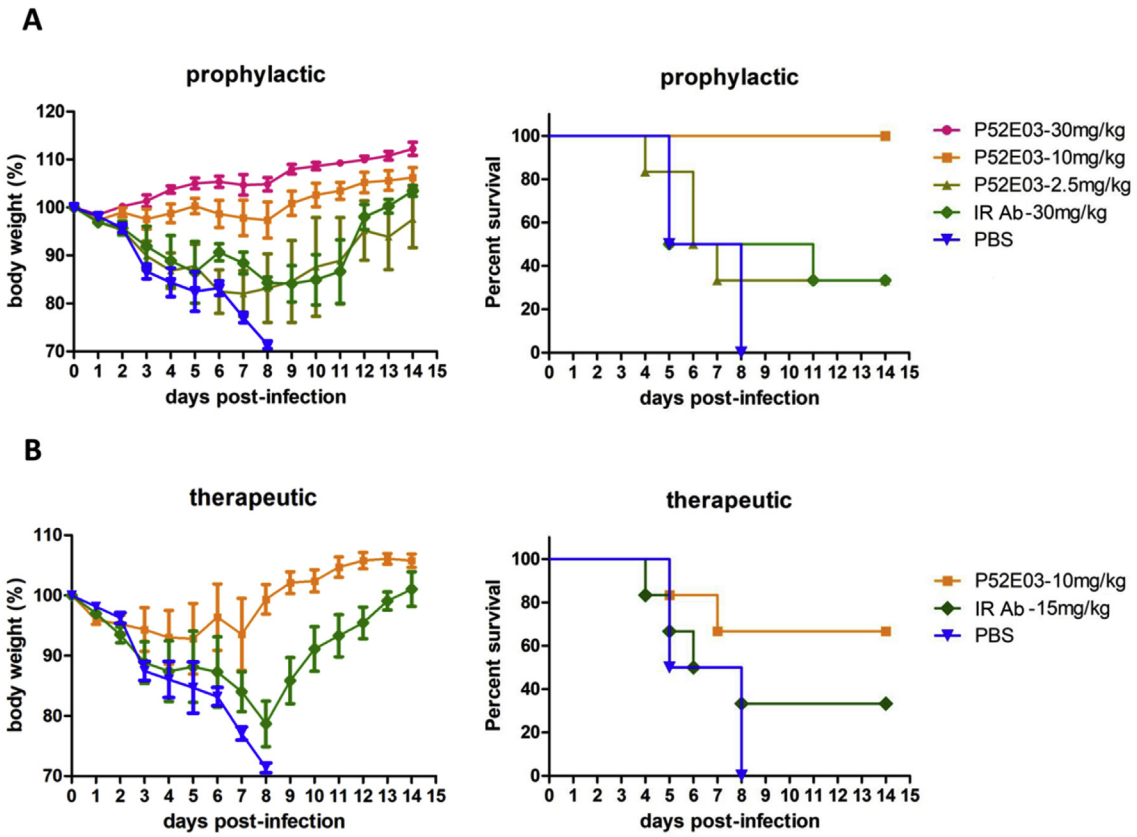

Fig. 7. Prophylactic and therapeutic efficacy in the mouse model. *In vivo* prophylactic (A) and therapeutic (B) efficacy of P52E03 against 10 LD_{50} NIBRG-267(H7N9) viruses. A single dose of antibody or control was administered 24 h before and after intranasal infection in the prophylactic and therapeutic experiment, respectively. PBS and irrelevant antibody (IR Ab) were used as controls. Body weight data are shown as group mean ± s.e.m. of the percent in weight of surviving animals relative to their initial weight.

66.7% under the latter conditions (Fig. 7B). This finding suggested that P52E03 exerted a higher protective efficacy when administrated prophylactically than therapeutically. Mock control mice (PBS group) continued to lose weight and succumbed to infection by day 8. Mice that received an irrelevant mAb (NiV41, which is specific for Nipha virus) but not H7-reactive mAb started to lose weight soon after viral infection and the survival rate was 33.3%.

4. Discussion

Here we identified a human antibody, P52E03, capable of neutralizing divergent H7 viruses belonging to both North American and Eurasian lineages *in vitro*. We characterized its epitope by generating escape mutant variants and found that G151 is a key residue for antibody binding. A similar variant has been selected by the murine antibody 1B2, containing two simultaneous mutations, S150L and G151E [Tan et al, 2016]. Three flanking residues, R149, S152, and S153, have been found to be vital for HI activity of the human antibodies 07-4D05, 07-4B03, and 07-4E02, respectively [Henry Dunand et al, 2016]. The R149 site was also critical for the murine antibodies 5A6, 2C4, 4A2, and 1A8 [Schmeisser et al, 2015; Tan et al, 2016]. All these antibodies showed cross-reactivity to divergent H7 viruses, and the five key residues are composition of antigenic site A (148–153, RRSGSS), which is highly conserved in H7 protein. Among 4395 full-length H7 proteins from GISAID, the percentage of substitution for each residue was low, i.e., R149G (0), S150L (0.84%), G151E (0.86%), S152P (1.77%) and S153P (0), suggesting that antigenic site A was highly conserved and, therefore, antibodies targeting this site may exert cross-reactivity to divergent H7 viruses. For another mAb L3A-44, whose crystal structure has been determined, interacts residues in site A including G151 and site B [Huang et al., 2018a]. We notice that the spectra for neutralizing of our antibody P52E03 and mAb L3A-44 are different. The possible reason could be that P52E03 recognizes residues mostly in and around site A as analysis of escape mutant variants and computational predication.

It is important to determine whether antigenic site A is vulnerable to the human immune system. Unlike the anti-stem antibody CR6261, whose germline precursor only engaged HA when expressed as cell surface IgM [Lingwood et al, 2012], we found that the germline precursors of both P52E03 and 07-4B03 bound HA as soluble IgGs with measurable affinity, and their epitopes may be more vulnerable to the immune system. According to a study on broadly neutralizing antibodies against subtype H1 influenza viruses, immunogens selectively exposing conserved epitopes might be a constructive step toward the design of broad-spectrum vaccines [Schmidt et al, 2015]. Thus, it might be possible to design a broad-spectrum H7 vaccine by using priming vaccine antigens to activate B cells targeting conserved H7 antigenic sites, followed by vaccination with a series of slightly different antigens to drive affinity maturation.

In summary, we have shown a human antibody, P53E03, targeting H7 antigenic site A with a new key residue (G151) and showed cross-HI and -MN activity against divergent H7 viruses of North American and Eurasian lineages. Those conserved residues, in and around antigenic site A, compose an ideal epitope for developing cross-reactive binding antibodies and vaccines against divergent H7 viruses.

Acknowledgments

We are thankful to The Core Facility and Technical Support, Wuhan Institute of Virology, Chinese Academy of Sciences (Xuefang An, Hao

Tang, Yuzhou Xiao, Youling Zhu and Fan Zhang for assistance with the mice experiments, and Ding Gao for the technical assistance on BLI experiment); Wuhan Key Laboratory on Emerging Infectious Diseases and Biosafety; as well as Wuhan National Bio-Safety Level 4 Lab of the Chinese Academy of Sciences for the supports.

This work was funded by the China Mega-Project for Infectious Disease (2017ZX10103005-005), the National Key Technology R&D Program of China (2017ZX10104001) and the External Cooperation Program of Chinese Academy of Sciences (153211KYSB20160001).

Appendix A. Supplementary data

Supplementary data to this article can be found online at https://doi.org/10.1016/j.antiviral.2019.104556.

References

Team, E, 2007. Avian influenza A/(H7N2) outbreak in the United Kingdom. Wkly. Releases 12 (22), 3206. 1997–2007. https://doi.org/10.2807/esw.12.22.03206-en.

Abdelwhab, E.M., Veits, J., Mettenleiter, T.C., 2014. Prevalence and control of H7 avian influenza viruses in birds and humans. Epidemiol. Infect. 142 (5), 896–920. https://doi.org/10.1017/S0950268813003324.

Aoki, F.Y., et al., 2003. Early administration of oral oseltamivir increases the benefits of influenza treatment. J. Antimicrob. Chemother. 51 (1), 123–129. https://doi.org/10.1093/jac/dkg007.

Banks, J., Speidel, E.C., McCauley, J.W., Alexander, D.J., 2000. Phylogenetic analysis of H7 haemagglutinin subtype influenza A viruses. Arch. Virol. 145 (5), 1047–1058. https://doi.org/10.1007/s007050050695.

Bart, S.A., Hohenboken, M., Della Cioppa, G., Narasimhan, V., Dormitzer, P.R., Kanesa-Thasan, N., 2014. A cell culture-derived MF59-adjuvanted pandemic A/H7N9 vaccine is immunogenic in adults. Sci. Transl. Med. 6 (234), 234ra255. https://doi.org/10.1126/scitranslmed.3008761.

Burke, D.F., Smith, D.J., 2014. A recommended numbering scheme for influenza a HA subtypes. PLoS One. https://doi.org/10.1371/journal.pone.0112302.t001.

CDC, 2004a. Centers for disease control and prevention. Update: influenza activity—United States, 2003–04 season. MMWR Morb. Mortal. Wkly. Rep. 53, 284–287 2004.

CDC, 2004b. Centers for Disease Control and Prevention. Update: influenza activity—United States and worldwide, 2003–04 season, and composition of the 2004–05 influenza vaccine. MMWR Morb. Mortal. Wkly. Rep. 53, 547–552 2004.

Chaudhury, S., Berrondo, M., Weitzner, B.D., Muthu, P., Bergman, H., Gray, J.J., 2011. Benchmarking and analysis of protein docking performance in Rosetta v3.2. PLoS One 6 (8). https://doi.org/10.1371/journal.pone.0022477. e22477-e22477.

Dreyfus, C., et al., 2012. Highly conserved protective epitopes on influenza B viruses. Science 337 (6100), 1343–1348. https://doi.org/10.1126/science.1222908.

Fabiani, C., Donatelli, I., Campitelli, L., Puzelli, S., Di Trani, L., De Marco, M.A., Capua, I., Aguilera, J.F., Zambon, M., 2005. Serological analysis of serum samples from humans exposed to avian H7 influenza viruses in Italy between 1999 and 2003. J. Infect. Dis. 192 (8), 1318–1322. https://doi.org/10.1086/444390.

Fries, L.F., Smith, G.E., Glenn, G.M., 2013. A recombinant viruslike particle influenza a (H7N9) vaccine. N. Engl. J. Med. 369 (26), 2564–2566. https://doi.org/10.1056/NEJMc1313186.

Gao, R., et al., 2013. Human infection with a novel avian-origin influenza a (H7N9) virus. N. Engl. J. Med. 368 (20), 1888–1897. https://doi.org/10.1056/NEJMoa1304459.

Goff, P.H., Krammer, F., Hai, R., Seibert, C.W., Margine, I., Garcia-Sastre, A., Palese, P., 2013. Induction of cross-reactive antibodies to novel H7N9 influenza virus by recombinant Newcastle disease virus expressing a North American lineage H7 subtype hemagglutinin. J. Virol. 87 (14), 8235–8240. https://doi.org/10.1128/JVI.01085-13.

Henry Dunand, C.J., et al., 2016. Both neutralizing and non-neutralizing human H7N9 influenza vaccine-induced monoclonal antibodies confer protection. Cell Host Microbe 19 (6), 800–813. https://doi.org/10.1016/j.chom.2016.05.014.

Hoffmann, E., Neumann, G., Kawaoka, Y., Hobom, G., Webster, R.G., 2000. A DNA transfection system for generation of influenza A virus from eight plasmids. Proc. Natl. Acad. Sci. U. S. A 97 (11), 6108–6113. https://doi.org/10.1073/pnas.100133697.

Huang, K.A., et al., 2018a. Structure-function analysis of neutralizing antibodies to H7N9 influenza from naturally infected humans. Nat. Microbiol. https://doi.org/10.1038/s41564-018-0303-7.

Jackson, L.A., et al., 2015. Effect of varying doses of a monovalent H7N9 influenza vaccine with and without AS03 and MF59 adjuvants on immune response: a randomized clinical trial. J. Am. Med. Assoc. 314 (3), 237–246. https://doi.org/10.1001/jama.2015.7916.

Jie, D., Bo, P., Sheng-bo, H., Jing-jing, T., Xiao-man, L., Fang, F., Feng-hua, Z., Hai-yan, C., 2016. Comparison of several adjuvants for inactivated H7N9 influenza virus vaccine. Chin. Prev. Med. 17 (0009).

Ke, C., et al., 2017. Human infection with highly pathogenic avian influenza A(H7N9) virus, China. Emerg. Infect. Dis. 23 (8), 1332–1340. https://doi.org/10.3201/eid2308.170600.

Klausberger, M., Wilde, M., Palmberger, D., Hai, R., Albrecht, R.A., Margine, I., Hirsh, A., García-Sastre, A., Grabherr, R., Krammer, F., 2014. One-shot vaccination with an insect cell-derived low-dose influenza A H7 virus-like particle preparation protects mice against H7N9 challenge. Vaccine 32 (3), 355–362. https://doi.org/10.1016/j.vaccine.2013.11.036.

Koopmans, M., et al., 2004. Transmission of H7N7 avian influenza A virus to human beings during a large outbreak in commercial poultry farms in The Netherlands. The Lancet 363 (9409), 587–593. https://doi.org/10.1016/S0140-6736(04)15589-X.

Krammer, F., et al., 2014. Divergent H7 immunogens offer protection from H7N9 virus challenge. J. Virol. 88 (8), 3976–3985. https://doi.org/10.1128/JVI.03095-13.

Krause, J.C., et al., 2012. Human monoclonal antibodies to pandemic 1957 H2N2 and pandemic 1968 H3N2 influenza viruses. J. Virol. 86 (11), 6334–6340. https://doi.org/10.1128/JVI.07158-11.

Lingwood, D., McTamney, P.M., Yassine, H.M., Whittle, J.R., Guo, X., Boyington, J.C., Wei, C.J., Nabel, G.J., 2012. Structural and genetic basis for development of broadly neutralizing influenza antibodies. Nature 489 (7417), 566–570. https://doi.org/10.1038/nature11371.

Liu, S., Li, M., Su, Z., Deng, F., Chen, J., 2016. A 3-year follow-up study of the seroprevalence of antibodies to avian influenza A H5, H6, H7 and H10 viruses among the general population of Wuhan, China. J. Clin. Virol. 77, 109–110. https://doi.org/10.1016/j.jcv.2016.02.018.

Marcatili, P., et al., 2008. PIGS: automatic prediction of antibody structures. Bioinformatics. https://doi.org/10.1093/bioinformatics/btn341.

Margine, I., Palese, P., Krammer, F., 2013. Expression of functional recombinant hemagglutinin and neuraminidase proteins from the novel H7N9 influenza virus using the baculovirus expression system. J. Vis. Exp. 81, e51112. https://doi.org/10.3791/51112.

Mulligan, M.J., et al., 2014. Serological responses to an avian influenza A/H7N9 vaccine mixed at the point-of-use with MF59 adjuvant: a randomized clinical trial. J. Am. Med. Assoc. 312 (14), 1409–1419. https://doi.org/10.1001/jama.2014.12854.

Nguyen-Van-Tam, J.S., et al., 2006. Outbreak of low pathogenicity H7N3 avian influenza in UK, including associated case of human conjunctivitis. Wkly. Releases 11 (18), 2952. https://doi.org/10.2807/esw.11.18.02952-en 1997-2007.

Pedotti, M., Simonelli, L., Livoti, E., Varani, L., 2011. Computational docking of antibody-antigen complexes, opportunities and pitfalls illustrated by influenza hemagglutinin. Int. J. Mol. Sci. 12 (1), 226–251. https://doi.org/10.3390/ijms12010226.

Poland, G.A., Ovsyannikova, I.G., Jacobson, R.M., 2009. Influenza virus resistance to antiviral agents: a plea for rational use. Clin. Infect. Dis. 48 (9), 1254–1256. https://doi.org/10.1086/598989.

Schmeisser, F., Vasudevan, A., Verma, S., Wang, W., Alvarado, E., Weiss, C., Atukorale, V., Meseda, C., Weir, J.P., 2015. Antibodies to antigenic site A of influenza H7 hemagglutinin provide protection against H7N9 challenge. PLoS One 10 (1), e0117108. https://doi.org/10.1371/journal.pone.0117108.

Schmidt, A.G., Do, K.T., McCarthy, K.R., Kepler, T.B., Liao, H.X., Moody, M.A., Haynes, B.F., Harrison, S.C., 2015. Immunogenic stimulus for germline precursors of antibodies that engage the influenza hemagglutinin receptor-binding site. Cell Rep. 13 (12), 2842–2850. https://doi.org/10.1016/j.celrep.2015.11.063.

Schneidman-Duhovny, D., Inbar, Y., Nussinov, R., Wolfson, H.J., 2005. PatchDock and SymmDock: servers for rigid and symmetric docking. Nucleic Acids Res. 33, W363–W367. https://doi.org/10.1093/nar/gki481.

Sergey, L., Gray, J.J., 2008. The RosettaDock server for local protein–protein docking. Nucleic Acids Res. 36 (Suppl. l_2), W233–W238. https://doi.org/10.1093/nar/gkn216.

Sergey, L., et al., 2013. Serverification of molecular modeling applications: the Rosetta online server that includes everyone (ROSIE). PLoS One 22 (8), e63906. https://doi.org/10.1371/journal.pone.0063906. 5.

Sparrow, E., Friede, M., Sheikh, M., Torvaldsen, S., Newall, A.T., 2016. Passive immunization for influenza through antibody therapies, a review of the pipeline, challenges and potential applications. Vaccine 34 (45), 5442–5448. https://doi.org/10.1016/j.vaccine.2016.08.057.

Su, S., Gu, M., Liu, D., Cui, J., Gao, G.F., Zhou, J., Liu, X., 2017. Epidemiology, evolution, and pathogenesis of H7N9 influenza viruses in five epidemic waves since 2013 in China. Trends Microbiol. 25 (9), 713–728. https://doi.org/10.1016/j.tim.2017.06.008.

Tan, G.S., Leon, P.E., Albrecht, R.A., Margine, I., Hirsh, A., Bahl, J., Krammer, F., 2016. Broadly-reactive neutralizing and non-neutralizing antibodies directed against the H7 influenza virus hemagglutinin reveal divergent mechanisms of protection. PLoS Pathog. 12 (4), e1005578. https://doi.org/10.1371/journal.ppat.1005578.

Thornburg, N.J., et al., 2016. H7N9 influenza virus neutralizing antibodies that possess few somatic mutations. J. Clin. Investig. 126 (4), 1482–1494. https://doi.org/10.1172/JCI85317.

Tweed, S.A., et al., 2004. Human illness from avian influenza H7N3, British Columbia. Emerg. Infect. Dis. 10 (12), 2196–2199. https://doi.org/10.3201/eid1012.040961.

WHO, 2017. Antigenic and Genetic Characteristics of Zoonotic Influenza Viruses and Development of Candidate Vaccine Viruses for Pandemic Preparedness. 201709.

WHO, 2018. Human Infection with Avian Influenza A(H7N9) Virus -The Total Number of Fatal Cases Is Published on a Monthly Basis by the China National Health and Family Planning Commission.

WHO, 2019. Antigenic and Genetic Characteristics of Zoonotic Influenza Viruses and Development of Candidate Vaccine Viruses for Pandemic Preparedness. pp. 201902.

Wiley, D.C., Wilson, I.A., Skehel, J.J., 1981. Structural identification of the antibody-binding sites of Hong Kong influenza haemagglutinin and their involvement in antigenic variation. Nature 289 (5796), 373–378. https://doi.org/10.1038/289373a0.

Xiao, X., Chen, W., Feng, Y., Zhu, Z., Prabakaran, P., Wang, Y., Zhang, M.Y., Longo, N.S., Dimitrov, D.S., 2009. Germline-like predecessors of broadly neutralizing antibodies lack measurable binding to HIV-1 envelope glycoproteins: implications for evasion of immune responses and design of vaccine immunogens. Biochem. Biophys. Res. Commun. 390 (3), 404–409. https://doi.org/10.1016/j.bbrc.2009.09.029.

Zhu, Z., Dimitrov, D.S., 2009. Construction of a large naive human phage-displayed Fab library through one-step cloning. Methods Mol. Biol. 525, 129–142. https://doi.org/10.1007/978-1-59745-554-1_6. xv.
Xu, R., et al., 2013. Preferential recognition of avian-like receptors in human influenza A H7N9 viruses. Science. https://doi.org/10.1126/science.1243761.
Zhu, Z., et al., 2006. Potent neutralization of Hendra and Nipah viruses by human monoclonal antibodies. J. Virol. 80 (2), 891–899. https://doi.org/10.1128/JVI.80.2.891-899.2006.
Zhu, Z., Prabakaran, P., Chen, W., Broder, C.C., Gong, R., Dimitrov, D.S., 2013. Human monoclonal antibodies as candidate therapeutics against emerging viruses and HIV-1. Virol. Sin. 28 (2), 71–80. https://doi.org/10.1007/s12250-013-3313-x.